Science of the Total Environment 557–558 (2016) 248–256

Contents lists available at ScienceDirect

Science of the Total Environment

journal homepage: www.elsevier.com/locate/scitotenv

Radionuclides in ornithogenic sediments as evidence for recent warming in the Ross Sea region, Antarctica

Yaguang Nie [a,b], Liqiang Xu [c], Xiaodong Liu [a,*], Steven D. Emslie [d]

[a] Institute of Polar Environment, School of Earth and Space Sciences, University of Science and Technology of China, Hefei 230026, China
[b] Key Laboratory of Ion Beam Bioengineering, Hefei Institutes of Physical Science, Chinese Academy of Sciences, Key Laboratory of Environmental Toxicology and Pollution Control Technology of Anhui Province, Hefei, Anhui 230031, China
[c] School of Resources and Environmental Engineering, Hefei University of Technology, Hefei, Anhui 230009, China
[d] Department of Biology and Marine Biology, University of North Carolina Wilmington, 601 S. College Road, Wilmington, NC 28403, USA

HIGHLIGHTS

- ^{210}Pb, ^{226}Ra and ^{137}Cs were measured in ornithogenic sediment profiles.
- Chronology within 200 years was determined through Constant Rate of Supply model.
- Calculated nuclide fluxes decreased with average deposition rate and locations.
- Deposition rate over time indicated warming which caused the flux gradient.

GRAPHICAL ABSTRACT

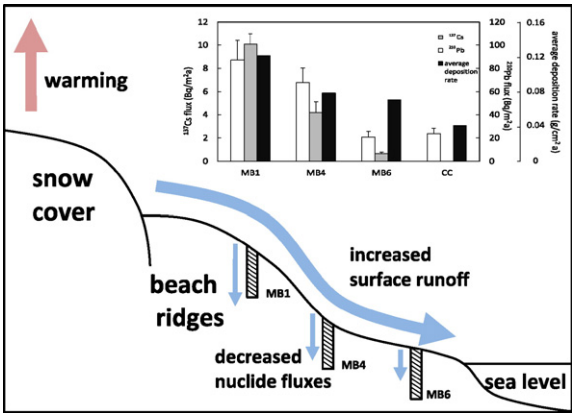

ARTICLE INFO

Article history:
Received 16 November 2015
Received in revised form 5 March 2016
Accepted 8 March 2016
Available online 19 March 2016

Editor: F. Riget

Keywords:
Radionuclides
^{210}Pb dating
^{210}Pb and ^{137}Cs flux
Ornithogenic sediments
Climate warming
Ross Sea region

ABSTRACT

Radionuclides including ^{210}Pb, ^{226}Ra and ^{137}Cs were analyzed in eight ornithogenic sediment profiles from McMurdo Sound, Ross Sea region, East Antarctica. Equilibration between ^{210}Pb and ^{226}Ra were reached in all eight profiles, enabling the determination of chronology within the past two centuries through the Constant Rate of Supply (CRS) model. Calculated fluxes of both ^{210}Pb and ^{137}Cs varied drastically among four of the profiles (MB4, MB6, CC and CL2), probably due to differences in their sedimentary environments. In addition, we found the flux data exhibiting a clear decreasing gradient in accordance with their average deposition rate, which was in turn related to the specific location of the profiles. We believe this phenomenon may correspond to global warming of the last century, since warming-induced surface runoff would bring more inflow water and detritus to the coring sites, thus enhancing the difference among the profiles. To verify this hypothesis, the deposition rate against age of the sediments was calculated based on their determined chronology, which showed ascending trends in all four profiles. The significant increase in deposition rates over the last century is probably attributable to recent warming, implying a potential utilization of radionuclides as environmental indicators in this region.

* Corresponding author.
E-mail address: ycx@ustc.edu.cn (X. Liu).

http://dx.doi.org/10.1016/j.scitotenv.2016.03.046
0048-9697/

1. Introduction

The radiometric dating method on shorter time scales (less than 200 years ago) using the natural fallout radionuclide ^{210}Pb was initially introduced by Goldberg (1963), but it was not widely used until after its first application to lake sediments by Krishnaswamy et al. (1971). Later with the development of calculation models of Constant Initial Concentration (CIC, for uniform accumulation rate) and Constant Rate of Supply (CRS, for non-uniform accumulation rate), and corroboration from artificial fallout radionuclides including ^{137}Cs and ^{241}Am for accurate age calibration (Appleby and Oldfield, 1978), the dating method broadened its usage into different geo-carriers such as lake, estuarine and marine sediments, and peat bogs (Appleby, 2008). After decades of application, ^{210}Pb dating has been recognized as one of the most important dating techniques in various paleo studies.

So far, studies on natural and artificial fallout radionuclides in Antarctica serve diverse purposes besides dating. For example, analyses of natural and artificial radionuclides on different materials including ice, sediments, soils, seawater, and biological samples play important roles in establishing baselines from which to estimate the possible impacts of radioactive pollution, to understand marine dynamic processes, and to examine the impacts of anthropogenic activities on this remote area (Schüller et al., 2004; Sanders et al., 2010). Radionuclides in aqueous systems may function as tracers for investigating water circulation and sedimentary processes due to their distinctly different geochemical behaviors (Godoy et al., 1998). Historical records of radionuclides have been used to study the long range water and atmospheric transportation of anthropogenic substances, and for exploring mineral resources (Jia et al., 2000). Snow-firn-ice dynamics based on ^{210}Pb deposition could grant insights into the balance of the Antarctic ice sheet (Goodwin, 1990; Gallée et al., 2001).

Antarctica developed its own unique ecosystem structures due to its isolation from other continents and the absence of anthropogenic influence (Jenouvrier et al., 2005). Its specific location and fragile ecosystems make this land extremely sensitive to climate change (Clarke et al., 2007). In the coastal ice-free areas scattered around Antarctica where migrating birds have the most impact, continuous and well-preserved ornithogenic sediments were formed, and serve as a natural archive for both geochemical dynamics and paleo-environmental conditions, allowing studies on climate change and the corresponding ecological responses in the past, which, in turn, is essential in understanding current and future trends of global warming and its impact on local ecosystems (Parmesan, 2006; McClintock et al., 2008). The Ross Sea is a high latitude embayment with a long history of Adélie penguin (*Pygoscelis adeliae*) occupation (Emslie et al., 2007). Our previous studies focused mainly on the geochemical features and processes based on heavy metal mercury, bio-element assemblage, stable isotope δ^{13}C and δ^{15}N, and rare earth elements in the ornithogenic sediments from this region (Nie et al., 2015). To further decode the information of the past stored in the sediments, accurate chronology of these ornithogenic sediments is crucially required.

In this study, we analyzed the levels of radionuclides including ^{210}Pb, ^{226}Ra and ^{137}Cs in eight ornithogenic sediment profiles collected from the ice-free areas in McMurdo Sound of the Ross Sea region for the first time. Since no data on radionuclides on a similar geo-carrier was ever reported in this area, we wished to determine whether the sediments with heavy avian influence could be used for ^{210}Pb dating, and exploit the potential of the radionuclides as indicators for environment change.

2. Material and methods

2.1. Study area

Ornithogenic sediments used in this study were collected in ice-free areas of the southern Ross Sea region in January 2010 (Fig. 1). This region is highly sensitive to climate change as it is located at the conjunction of three different air masses from Victoria Land, the Ross Sea, and the Ross Ice Shelf. The weather here is capricious and severe: the mean annual temperature is −18 °C, and the temperature may reach 8 °C in summer and −50 °C in winter. The average wind speed is 22.8 km/h, but may exceed 190 km/h on occasion. Ross Island (~2460 km^2) is of volcanic origin in McMurdo Sound comprising four volcanoes: Mts Terror (elevation: 3262 m,), Terra Nova (2130 m), Erebus (3794 m), and Bird (1800 m), with glacial ice mantles inland, leaving three ice-free areas where Adélie penguins currently breed at Cape Crozier (~18 km^2), Cape Bird (~15 km^2), and Cape Royds (~13 km^2). Beaufort Island (~18.4 km^2) is 21 km north of Ross Island with Adélie penguins breeding on the ice-free areas on the eastern and southern coasts. A long history of penguin occupation has left these areas with numerous abandoned penguin colonies as well as active ones, allowing the study of penguin paleoecology. Surface run-offs are observed in summers, and with the input of nutrients from penguin guano, freshwater algae are widely distributed in the ponds and catchments near the colonies.

2.2. Sample collection

The sampling sites are located in several separate areas on Ross and Beaufort Islands (Fig. 1). Details on depth, location, lithology (see also Supplementary Fig. 1) and catchment description of the eight profiles are provided in Table 1. The site MB4 is close to abandoned penguin colonies in mid Cape Bird. MB4 was collected in a small pond between the fourth and fifth raised beach ridges. According to field observations, the sediment layer below 15 cm was comprised of fine-grained ornithogenic sediments with a dark color and rancid smell; the sediment unit between 5 and 15 cm was mainly composed of dark-colored coarse sands; the surface layer is rich in fine black algae residue. Near MB4, profile CL2 was taken from the northern edge of a pond located on the fifth beach ridge above sea level. CL2 mostly consisted of fairly homogeneous black and grey colored silts, and its uppermost part was comprised of dark green freshwater algae residues. Profile MB6 was collected from a small catchment on the second terrace above sea level in an active penguin colony on the north side of Cape Bird. The sediments below 24 cm were dark-colored ornithogenic soils, and the remainder consisted of brown clay. Seal hairs were found in the sediment layer beneath 32 cm. Profile MB1 with relatively homogeneous lithology was collected from a dried-out catchment on an elevated hillside south of MB4 with traces of penguin activities (bones and feather discovered). Profile CC was collected from a fecal pit in Cape Crozier, Ross Island. Large amounts of penguin guano were deposited here, together with eggshells and downy feathers. The biological remains were concentrated in the layer above 7 cm. Profile MR1 and MR2 were collected near the active penguin colonies at Cape Royds. From bottom to top, both profiles changed from dark-colored weathering products to red-colored ornithogenic sediments with gravels at critical depths of 12 and 15 cm, respectively. Profile BI was excavated from a small peat near the modern penguin colony on the southwest side of Beaufort Island. From the bottom to top, brown clay gradually transitions into black fine-grained ornithogenic sediments. Profile MB4, MB6, MB1, MR1 and MR2 were directly taken in dug pits and sectioned in the field (intervals: 0.8 cm for MB4; 0.6 cm for MB6; 1 cm for MB1, 1 cm for layer above 15 cm, 2 cm for layer below 15 cm in MR1; 1 cm for layer above 15 cm, 2 cm for layer below 15 cm, and the remaining sediments were divided into 2 subsamples in MR2), while CC, BI and CL2 were collected using sediment cores and transported back to the lab and sectioned at the intervals of 0.5 cm. All sediment samples were air dried and homogenized by grinding before radionuclide and chemical analyses. More details about sampling have been reported in Nie et al. (2012, 2015).

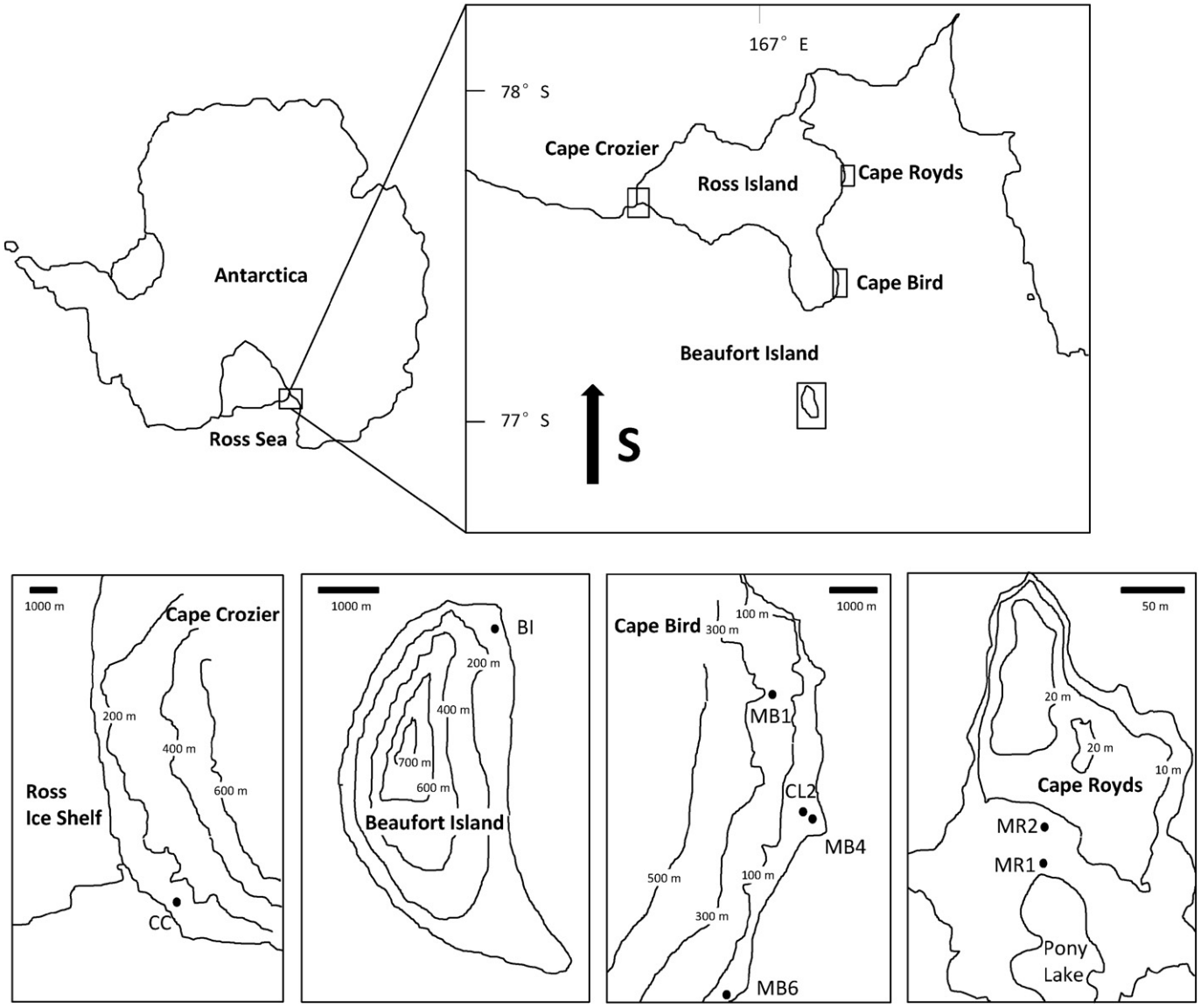

Fig. 1. The study area and the sampling sites in the Ross Sea region.

2.3. Analytical methods

The radioactivity of sediment samples was measured by direct gamma spectrometry (Ortec HPGe GWL series, well-type, coaxial, low background, intrinsic germanium detector, AMETEK Company). The detector was protected by a 2 mm inner copper wall and a 10 cm outer lead chamber (connected to a liquid nitrogen tank for thermal stability) to avoid possible interference of background radiation. The standard radionuclide samples (soil samples) were provided and calibrated by the China Institute of Atomic Energy (isotopes for calibration: ^{210}Pb, ^{226}Ra, ^{137}Cs, ^{241}Am, ^{155}Eu, ^{57}Co, ^{54}Mn, ^{65}Zn and ^{60}Co). Homogenized sediment samples were dried at 105 °C to constant weight and sealed into 5 ml centrifuge tubes for a storage of about 3 weeks to reach radioactive equilibration between ^{226}Ra and its daughter nuclide ^{214}Pb. Spectra

Table 1
Sampling information on the ornithogenic sediments from the Ross Sea region.

Profile	Depth (cm)	Location	Coordinates	Lithology		Catchment
				Guano	Algae	
MB4	42	Cape Bird, Ross Island	166° 22′ 25.6″ E, 77° 14′ 35.3″ S	Moderate	Major	Large
CL2	35	Cape Bird, Ross Island	166° 22′ 25.6″ E, 77° 14′ 35.3″ S	Moderate	Minor	Large
MB6	38	Cape Bird, Ross Island	166° 26′ 44.4″ E, 77° 12′ 47.5″ S	Major	Major	Small
MB1	51	Cape Bird, Ross Island	166° 22′ 26″ E, 77° 14′ 35.7″ S	Moderate	None	Large
CC	9.5	Cape Crozier, Ross Island	169° 14′ 41.3″ E, 77° 27′ 21.9″ S	Major	None	Small
MR1	35	Cape Royds, Ross Island	166° 09′ 55.5″ E, 77° 33′ 15.2″ S	Major	None	Small
MR2	50	Cape Royds, Ross Island	166° 09′ 54.0″ E, 77° 33′ 16.1″ S	Major	None	Small
BI	20.5	Beaufort Island	166° 58′ 23.6″ E, 76° 58′ 23.6″ S	Major	Major	Small

Table 2
Activities of radionuclides in the ornithogenic sediments from the Ross Sea region.

Sample no.	Depth (cm)	Dry density (g/cm^3)	^{210}Pb activity (Bq/kg)	^{226}Ra activity (Bq/kg)	^{137}Cs activity (Bq/kg)
MB4-1	0.8	1.04	63.9 ± 8.2	28.7 ± 1.6	3.1 ± 0.9
MB4-2	1.6	1.15	74.5 ± 13.1	30.0 ± 1.8	4.1 ± 0.8
MB4-3	2.4	0.74	65.3 ± 11.2	30.6 ± 1.9	6.6 ± 1.0
MB4-4	3.2	0.88	75.6 ± 10.3	35.3 ± 1.9	5.3 ± 0.8
MB4-5	4	1.22	58.5 ± 12.0	38.2 ± 1.9	2.3 ± 0.6
MB4-6	4.8	1.49	67.0 ± 12.5	33.1 ± 2.1	1.7 ± 0.8
MB4-7	5.6	1.75	58.7 ± 9.7	40.1 ± 1.9	BDL
MB4-8	6.4	2.15	42.7 ± 8.7	37.3 ± 1.7	BDL
MB4-9	7.2	2.10	48.1 ± 9.1	44.3 ± 2.1	BDL
MB4-10	8	2.19	34.5 ± 6.3	36.0 ± 1.7	BDL
MB6-1	0.6	1.41	47.0 ± 9.6	34.8 ± 2.5	BDL
MB6-2	1.2	1.30	47.2 ± 11.6	30.3 ± 2.1	3.6 ± 0.9
MB6-3	1.8	1.66	45.2 ± 10.4	29.0 ± 2.0	BDL
MB6-4	2.4	1.46	56.6 ± 11.9	43.4 ± 2.6	BDL
MB6-5	3	1.40	40.8 ± 7.7	34.6 ± 2.0	BDL
MB6-6	3.6	1.43	43.9 ± 7.3	39.1 ± 2.2	BDL
MB6-7	4.2	1.38	25.9 ± 8.0	20.3 ± 1.4	BDL
MB6-8	4.8	1.43	35.1 ± 9.2	28.7 ± 2.0	BDL
MB6-9	5.4	1.66	33.3 ± 6.2	37.8 ± 2.2	BDL
CL2-1	0.5	1.10	76.0 ± 12.3	43.3 ± 2.1	2.8 ± 0.8
CL2-2	1	0.89	57.7 ± 11.6	40.9 ± 2.1	3.3 ± 0.9
CL2-3	1.5	1.41	67.6 ± 12.2	38.5 ± 1.8	1.1 ± 0.4
CL2-4	2	1.43	57.6 ± 11.8	38.3 ± 1.8	1.0 ± 0.4
CL2-5	2.5	1.56	63.5 ± 11.8	40.6 ± 2.0	1.3 ± 0.6
CL2-6	3	1.48	51.9 ± 8.2	42.1 ± 2.0	BDL
CL2-7	3.5	1.38	43.7 ± 7.9	40.7 ± 1.8	BDL
CL2-8	4	1.53	53.0 ± 9.3	46.6 ± 2.1	BDL
CL2-9	4.5	1.44	73.3 ± 12.5	47.7 ± 2.0	BDL
CL2-10	5	1.47	77.1 ± 14.6	46.8 ± 2.2	BDL
CL2-11	5.5	1.56	49.4 ± 7.9	32.8 ± 1.6	BDL
CL2-12	6	1.36	63.5 ± 11.4	33.7 ± 1.6	BDL
CL2-13	6.5	1.50	38.7 ± 7.9	30.0 ± 1.6	BDL
CL2-14	7	1.47	35.2 ± 8.2	33.9 ± 1.7	BDL
MB1-1	1	1.03	65.5 ± 10.7	11.6 ± 0.9	16.6 ± 1.1
MB1-2	2	1.40	41.0 ± 7.7	18.2 ± 1.3	14.6 ± 0.9
MB1-3	3	1.25	36.1 ± 6.2	12.7 ± 0.9	3.6 ± 0.6
MB1-4	4	1.35	44.8 ± 7.9	10.2 ± 0.8	1.4 ± 0.7
MB1-5	5	1.51	48.4 ± 8.7	19.8 ± 1.3	BDL
MB1-6	6	1.52	44.1 ± 8.4	18.3 ± 1.3	BDL
MB1-7	7	1.53	34.9 ± 6.6	20.6 ± 1.4	BDL
MB1-8	8	1.16	24.9 ± 5.1	17.8 ± 1.1	BDL
MB1-9	9	1.40	22.2 ± 6.0	19.0 ± 1.3	BDL
CC-1	0.5	0.70	36.0 ± 7.3	13.1 ± 1.1	BDL
CC-2	1	0.73	51.4 ± 8.9	25.2 ± 1.6	BDL
CC-4	2	0.71	48.8 ± 8.6	11.7 ± 0.9	BDL
CC-5	2.5	0.73	26.5 ± 5.0	6.8 ± 0.6	BDL
CC-6	3	0.73	32.5 ± 6.0	9.5 ± 0.8	BDL
CC-7	3.5	0.77	22.9 ± 4.7	2.8 ± 0.3	BDL
CC-8	4	0.75	12.7 ± 2.7	2.5 ± 0.3	BDL
CC-9	4.5	0.76	14.4 ± 3.0	7.4 ± 0.7	BDL
CC-10	5	0.75	15.6 ± 3.1	10.0 ± 0.7	BDL
MR1-1	1	/	95.8 ± 12.5	22.7 ± 1.5	2.0 ± 0.7
MR1-2	2	/	98.2 ± 8.3	22.4 ± 1.3	1.4 ± 0.8
MR1-3	3	/	129.7 ± 17.0	30.3 ± 2.1	1.7 ± 0.7
MR1-4	4	/	79.9 ± 11.7	21.8 ± 1.4	1.9 ± 0.5
MR1-5	5	/	55.9 ± 10.2	18.7 ± 1.4	2.0 ± 0.8
MR1-6	6	/	35.4 ± 6.4	22.9 ± 1.5	1.7 ± 0.8
MR1-7	7	/	46.7 ± 8.3	22.4 ± 1.7	BDL
MR1-8	8	/	61.4 ± 10.1	24.3 ± 1.6	BDL
MR1-9	9	/	40.5 ± 7.5	17.3 ± 1.0	BDL
MR1-10	10	/	28.2 ± 5.7	24.0 ± 1.8	BDL
MR2-1	1	/	76.5 ± 10.4	14.3 ± 1.0	BDL
MR2-2	2	/	90.6 ± 15.1	20.0 ± 1.6	BDL
MR2-3	3	/	72.3 ± 14.3	20.9 ± 1.8	BDL
MR2-4	4	/	74.9 ± 13.8	20.1 ± 1.6	BDL
MR2-5	5	/	76.9 ± 14.5	22.6 ± 2.0	BDL
MR2-6	6	/	26.6 ± 5.8	21.4 ± 1.7	BDL
MR2-7	7	/	89.8 ± 16.4	27.0 ± 2.4	BDL
MR2-8	8	/	47.8 ± 12.1	20.6 ± 1.7	BDL
MR2-9	9	/	45.6 ± 9.9	30.8 ± 2.3	BDL
MR2-10	10	/	31.2 ± 6.2	16.3 ± 1.5	BDL
BI-1	0.5	0.58	89.6 ± 15.0	28.0 ± 1.7	2.9 ± 1.2
BI-2	1	0.55	62.3 ± 10.0	28.0 ± 1.7	2.2 ± 0.7
BI-3	1.5	0.64	49.3 ± 9.6	30.4 ± 1.7	1.6 ± 0.8

(continued on next page)

Table 2 (*continued*)

Sample no.	Depth (cm)	Dry density (g/cm^3)	^{210}Pb activity (Bq/kg)	^{226}Ra activity (Bq/kg)	^{137}Cs activity (Bq/kg)
BI-4	2	0.81	40.8 ± 8.2	29.4 ± 1.7	3.5 ± 0.7
BI-5	2.5	0.66	34.8 ± 7.1	25.8 ± 1.7	BDL
BI-6	3	0.61	36.7 ± 7.2	29.6 ± 1.7	BDL
BI-7	3.5	0.74	42.8 ± 7.7	40.4 ± 2.1	BDL
BI-8	4	1.05	32.9 ± 5.8	31.9 ± 1.7	BDL

"/": not determined.
BLD: below detection limit.

were obtained after about 24 h to record sufficient counts. Activity of ^{210}Pb was measured by its peak at 46.5 keV in the resulting spectrum files. The ^{226}Ra activity was determined by its daughter isotope ^{214}Pb at 295 keV, and ^{137}Cs was measured by its emissions at 662 keV. Further details on this methodology can be found in Xu et al., 2010.

3. Results and discussion

3.1. Radionuclide distribution and chronology determination

^{210}Pb (half-life $T_{1/2}$ = 22.3 a) dating has been commonly used in lacustrine, marine and peat sediments based on the disequilibrium between ^{210}Pb and its parent isotope ^{226}Ra in the ^{238}U decay series, since part of the intermediate gaseous isotope ^{222}Rn would escape from the lithosphere to the atmosphere and join the circulation of air masses (Doran et al., 1999, Appleby, 2008; Le Roux and Marshall, 2011). Short-lived ^{222}Rn ($T_{1/2}$ = 3.8 d) then decays to ^{210}Pb and returns to the surface through wet and dry deposition. Local ^{210}Pb defined as supported ^{210}Pb is at equilibrium with ^{226}Ra, while precipitated ^{210}Pb defined as excess ^{210}Pb (^{210}Pb$_{ex}$) causes disequilibrium between ^{226}Ra and total ^{210}Pb. Since the decay of ^{210}Pb$_{ex}$ follows the radioactive decay law, time sequence of the upper layer sediments could thus be inferred from the half-life and concentration-versus-depth profiles of ^{210}Pb (Godoy et al., 1998).

Activity of radionuclides including ^{210}Pb, ^{226}Ra, ^{137}Cs in all eight profiles and the corresponding dry bulk density for each depth in the upper layers of MB4, MB6, MB1 and CC are given in Table 2. Nuclide data in profile MB4, MB6, CL2 and MB1 are concisely presented in the supplementary material of our previous study on the paleoecology (Nie et al., 2015), and here we discuss these data altogether with CC, MR1, MR2 and BI. ^{210}Pb and ^{226}Ra activities varied significantly among sites with the coefficient of variation for both nuclides around 40%. Since ^{210}Pb was generally declining due to the decay of ^{210}Pb$_{ex}$ and ^{226}Ra less fluctuating (Fig. 2), the difference of ^{226}Ra among profiles was more obvious. We tested the correlation between ^{226}Ra and grain size (median diameter) in MB4, MB6 CL2 and BI, and find it insignificant (data not shown). And finer sediments don't necessarily correspond to higher ^{226}Ra level (much lower median diameter in upper MB6 has similar ^{226}Ra level to CL2 with coarser grain size). Thus we believe ^{226}Ra was mainly determined by the lithological property of the bedrock that the sediments originally derived from. ^{210}Pb in MB4 was fluctuating with an overall monotonic decreasing trend, and met the slightly ascending ^{226}Ra at 8 cm (with the ^{210}Pb$_{ex}$ of more than 3 following subsamples around or below 0 for all eight profiles). Both ^{210}Pb and ^{226}Ra in MB6 formed a high value plateau from 2.4 to 3.6 cm, interrupting their decreasing trends. ^{226}Ra started to increase below the plateau while ^{210}Pb dropped at 4.8 cm, and ^{210}Pb$_{ex}$ reduced to its zero point at 5.4 cm. ^{210}Pb kept decreasing from the surface, but increased below 3.5 cm in CL2. Both ^{210}Pb and the stable ^{226}Ra started to decline below 5 cm with the equilibrium reached at 7 cm. ^{210}Pb in MB1 decreased sharply from surface to 3 cm in depth, then rose to a peak at 5 cm and went down gradually from there. ^{226}Ra in MB1 increased slowly but steadily, except for a minor drop at 4 cm, and the equilibration was reached at 9 cm. Both ^{210}Pb and ^{226}Ra in profile CC reached their maximum at 1 cm, and then declined and met their equilibrium at 5 cm. Besides the general descent in ^{210}Pb trends, both MR1 and MR2 showed a drop at 6 cm (more sudden in MR2), while ^{226}Ra was stable in the two profiles with their ^{210}Pb$_{ex}$ zero points at 10 cm. The smoothly decreasing ^{210}Pb in BI was disturbed by a minor peak at 3.5 cm, which was also observed in ^{226}Ra with the equilibrium reached right after at 4 cm.

Based on our field records and previous research on the geochemistry (Liu et al., 2013), the sediments are heavily impacted by avian activities. The organic matter (OM) consisted primarily of penguin guano and guano-nourished fresh-water algae, which might influence the nuclide in the surface layers. With this extra characteristic to normal lacustrine sediments, we need to determine the effect of OM on ^{210}Pb$_{ex}$ before age calculation. For all the profiles, guano and algae constitute the majority of total organic carbon (TOC), and phosphorus (P) serves as a robust marker for impact from penguin guano. To determine the extent of influence from guano and algae on ^{210}Pb$_{ex}$ distributions in the sediments, we analyzed the respective correlation of TOC and P with ^{210}Pb$_{ex}$. As can be seen in Table 3, there was little consistency in statistics with only MB4 and BI showing slight or moderate relationships to ^{210}Pb$_{ex}$-TOC and/or ^{210}Pb$_{ex}$-P, while the relationships in the other profiles were insignificant, indicating that OM cannot be a controlling factor for the distribution of ^{210}Pb$_{ex}$ in the bulk sediments. According to a previous study on the ornithogenic sediments from Xisha Islands, guano has much lower ^{210}Pb activity compared to the sediments, and does not exert much influence on the vertical distribution of ^{210}Pb$_{ex}$ (Xu et al., 2010). Similarly, ^{210}Pb activity in fresh guano and algae samples collected near the sediment profiles from the Ross Sea region were very low (^{210}Pb$_{guano}$ = 9.37 ± 4.22, n = 2; ^{210}Pb$_{algae}$ = 15.18 ± 2.63, n = 2). Considering the proportion of TOC in the profiles was usually around 5% or less (Liu et al., 2013), OM with low ^{210}Pb activity cannot be a source of ^{210}Pb$_{ex}$. As a function of nuclide activities of individual samples from depths, ^{210}Pb$_{ex}$ flux stands for a proxy for ^{210}Pb$_{ex}$ level. We listed ^{210}Pb$_{ex}$ flux in the sediments from several different sites around Antarctica in Table 5. According to the comparison, ^{210}Pb$_{ex}$ level in the ornithogenic sediments in our study was similar to that of Signy Island (ornithogenic), but higher than the lacustrine sediments unaffected by seabirds from the McMurdo Dry Valleys and South Shetland Islands. Thus we believe that guano and algae-derived organic matter may still act as an adsorbent and help in retaining the atmospherically deposited ^{210}Pb in the penguin-affected sediments. To sum up, the weak correlation ^{210}Pb$_{ex}$ showed with TOC and P for most of the eight profiles and the low ^{210}Pb activity in fresh guano and algae samples ruled out the possibility of guano or algae exerting heavy influence over the distribution of ^{210}Pb$_{ex}$. Alternatively, we suggest that ^{210}Pb in the sediments from this region was mainly controlled by atmospheric precipitation instead of OM, though OM does play a role in retaining ^{210}Pb in the sediments.

As shown in Fig. 2, ^{210}Pb in the measured profiles generally declined with depth, but not exponentially, probably attributed to the varying accumulation rate. With atmospheric fallout determined as the source of ^{210}Pb$_{ex}$, the Constant Rate of Supply (CRS) model was applied for dating calculations (Appleby, 2000; Appleby, 2008). The results of ^{210}Pb dating for all the profiles are plotted in Fig. 2. Accordingly, 6.4 cm in MB4, 4.2 cm in MB6, 6.5 cm in CL2, 8 cm in MB1, 4.5 cm in CC, 9 cm in MR1/MR2 and 3.5 cm in BI dated to 149, 119, 170, 135, 117, 151, 108 and 162 a, respectively.

^{137}Cs ($T_{1/2}$ = 30.2 a) is a radionuclide that originates solely from anthropogenic activities including nuclear/thermonuclear explosions

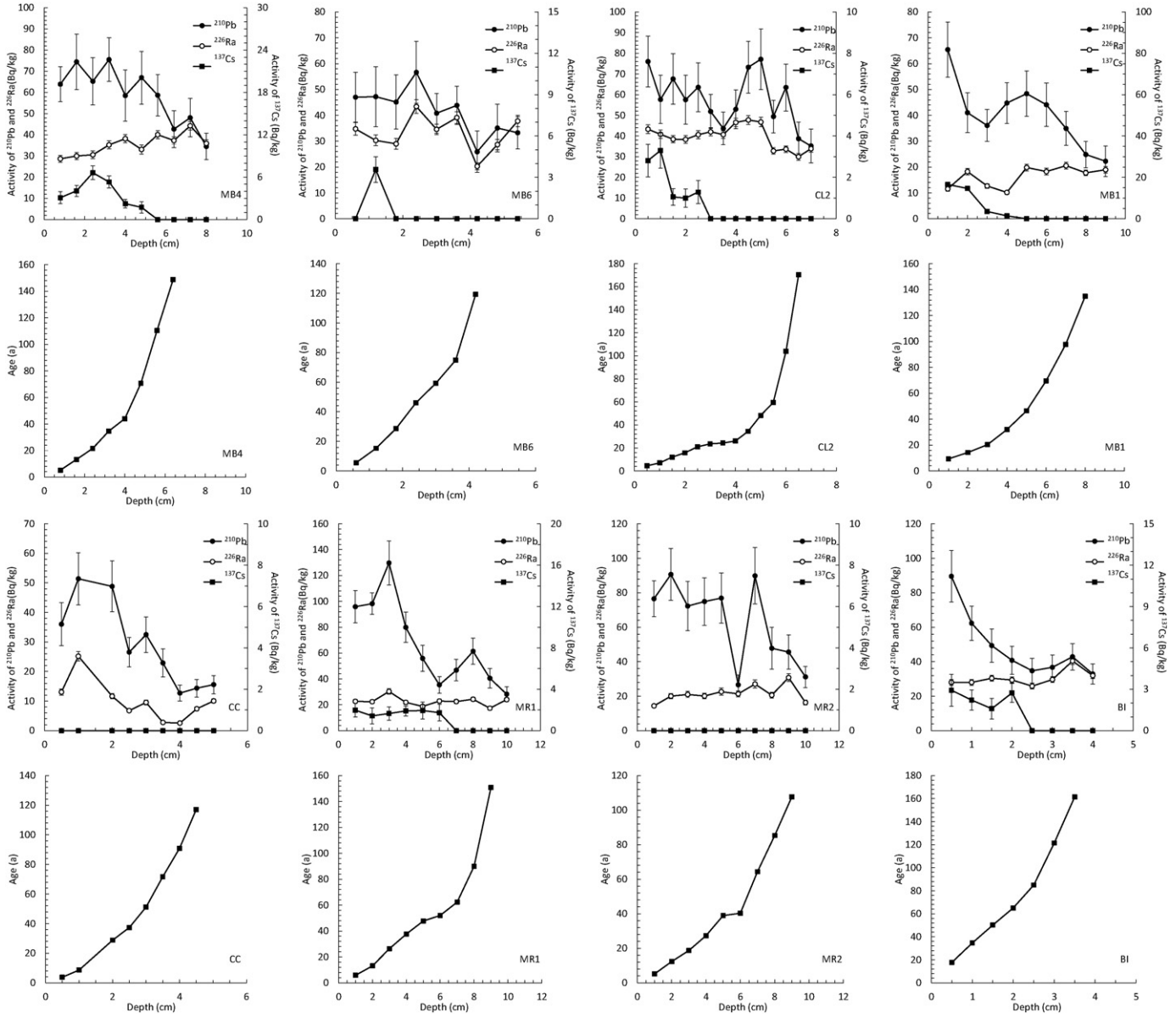

Fig. 2. Activities of ^{210}Pb, ^{226}Ra and ^{137} Cs against depth and results of dating using CRS model in the profiles.

(from 1950–1980s) and nuclear power plant accidents, which have occurred mainly in the Northern Hemisphere (Giuliani et al., 2003; Gulin and Stokozov, 2005). Though radioactive fallout tends to remain in the same hemisphere where it was produced, a small fraction of ^{137}Cs may still manage to slowly migrate to polar regions via global atmospheric circulation. The transit time for tropospheric transport of air masses from a distant continent to Antarctica is approximately 30 days (Maenhaut et al., 1979; UNSCEAR, 1982; Pourchet et al., 2003). Due to the precise time points marked by the nuclear tests and nuclear power plant accidents, deposited ^{137}Cs usually shows elevated activity in the corresponding layers, and thus can be used as a chronological marker to assist in the calibration of ^{210}Pb dates (Koide et al., 1979; Arnaud et al., 2006). The radionuclide was detected in most profiles, but the signal was generally weak (several Bq/kg, Table 2) except in profile MB1. From the surface layer to 4.8 cm in depth, ^{137}Cs in MB4 formed a peak with its maximum 6.6 Bq/kg at 2.4 cm. Throughout the profile of MB6, only the sediment sample at 1.2 cm showed ^{137}Cs activity of 3.6 Bq/kg. ^{137}Cs in CL2 was about 3 Bq/kg above 1 cm, then it declined to about 1 Bq/kg from 1 to 2.5 cm, and below which was undetectable. ^{137}Cs in MB1 dropped from 16.6 Bq/kg at 1 cm to 1.4 Bq/kg at 4 cm, and was not detected in the remaining section. All samples from CC and MR2 were below detection limit, while ^{137}Cs in MR2 fluctuated around 2 Bq/kg above 6 cm before dropping to 0 Bq/kg. ^{137}Cs in BI kept decreasing from the surface with depth, but formed a peak at the same level as the surface at 2 cm. The ^{137}Cs peak in MB4 was rather apparent at 1988, but judging from the fact that no signal

Table 3
Correlations between $^{210}Pb_{ex}$ and TOC, P in the profiles.

Profile	r^2 for TOC-$^{210}Pb_{ex}$	r^2 for P-$^{210}Pb_{ex}$
MB4	0.66[a] (n = 10)	0.20[b] (n = 7)
MB6	0.10[b] (n = 9)	0.046[b] (n = 3)
CL2	0.10[b] (n = 14)	0.01[b] (n = 8)
BI	0.57[a] (n = 8)	0.93[a] (n = 6)
CC	0.21[b] (n = 9)	0.56[b] (n = 4)
MB1	0.16[b] (n = 9)	0.0012[b] (n = 9)
MR1	0.17[b] (n = 10)	0.53[c] (n = 10)
MR2	0.028[b] (n = 10)	0.19[b] (n = 10)

[a] Significant at the 0.05 level.
[b] Not significant at the 0.05 level.
[c] Negative correlation significant at the 0.05 level.

Table 4
Calculated deposition rates, $^{210}Pb_{ex}$ and ^{137}Cs inventories and fluxes.

Profile	Average deposition rate (g/cm^2a)	$^{210}Pb_{ex}$ inventory (Bq/m^2)	$^{210}Pb_{ex}$ flux (Bq/m^2a)	^{137}Cs inventory (Bq/m^2)	^{137}Cs flux (Bq/m^2a)
MB1	0.1214	2801.56	87.24	439.14	10.09
MB4	0.0783	2181.11	67.92	182.56	4.19
MB6	0.0706	663.79	20.67	27.93	0.64
CC	0.0406	757.21	23.58	BDL	BDL

BLD: below detection limit.

of the Chernobyl nuclear plant accident has been detected in Antarctica, it is probably just the result of the high mobility of ^{137}Cs (de Lima Ferreira et al., 2013). ^{137}Cs in MR2 and CC was too low to function as a chronological marker, while its peaks in MB6, CL2, MR1 and BI were in discrepancy with ^{210}Pb age. This result may be explained by the following processes. First, the activity of the nuclide ^{137}Cs was greatly decreased due to the long distance transportation in the atmosphere. Very low levels of radioactivity in the sediments would weaken its function as a reference time marker. Second, the radionuclide ^{137}Cs is chemically active and has a relatively high mobility. Thus, downward diffusion might occur (Schüller et al., 2004; de Lima Ferreira et al., 2013). The surface layer in MB1 showed evident ^{137}Cs activity peaks, suggesting the local environment may impose a higher influence on the nuclide than precipitation (Schüller et al., 2004). ^{210}Pb dating in the Ross Sea region is relatively limited, however, analyzed nuclides from the ornithogenic sediments in this study produced sufficient data for ^{210}Pb dating. Due to the distant location of the sampling site, neither disturbance from human activities nor local animals were observed during field work. Further chronology determination using AMS ^{14}C dating based on biological remains including penguin bones/feathers and seal hairs showed no age inversion (Nie et al., 2015), reassuring the preservation of the sediments. Thus the reliability of ^{210}Pb dating of the ornithogenic sediments in the Ross Sea region can be validated.

3.2. Environmental implications of radionuclide flux in the Ross Sea region

Fluxes of $^{210}Pb_{ex}$ and ^{137}Cs in the profiles were calculated based on their inventories (I_s), which were in turn calculated from radioactivity and dry bulk density (measured only in MB4, MB6, MB1 and CC; Table 4) using the equations:

$$I_m = A \times \rho \times d$$
$$\text{flux} = I_s \times \lambda.$$

$I_m(Bq/m^2)$ was the individual inventory of the subsample at depth m calculated multiplying activity per weight unit (A: Bq/kg) by bulk density (ρ: g/cm^3) and the sectioning intervals (d: cm), and I_s (Bq/m^2) was total inventory of the profile (the add-up of I_m). The decay constant of ^{210}Pb $\lambda = 0.031\ a^{-1}$, and the decay constant of ^{137}Cs $\lambda = 0.023\ a^{-1}$. The result indicates $^{210}Pb_{ex}$ flux varying from 20.67 to 87.24 Bq/m^2a, and ^{137}Cs flux varying from 0.64 to 10.09 Bq/m^2a (Table 4). Compared to multiple $^{210}Pb_{ex}$ flux determined on different sources across Antarctica (Table 5), our results are similar to lacustrine sediments from Signy Island, since the profiles were developed in lacustrine or similar environments like the catchments near the penguin colonies. But $^{210}Pb_{ex}$ flux in the ornithogenic sediments was much greater than in some Antarctic lakes (only slightly higher than the value of direct fallouts from atmospheric precipitation, Table 5), which was probably caused by their limited catchment size. The calculated $^{210}Pb_{ex}$ and ^{137}Cs fluxes for the profiles MB1, MB4, MB6 and CC are given in Fig. 3. There is an evident difference among the profiles with the maximum more than 4× higher than the minimum $^{210}Pb_{ex}$ flux and 15× higher in ^{137}Cs (profile CC not included), and we found the inventory and flux in $^{210}Pb_{ex}$ and ^{137}Cs decreased in the order of MB1 > MB4 > MB6 > CC.

Since $^{210}Pb_{ex}$ and ^{137}Cs were both atmosphere-derived, precipitated nuclide fluxes should have a regional consistency (Godoy et al., 1998; Pourchet et al., 2003). However, the fluxes of the profiles varied significantly across Ross Island, implying a different mechanism. Thus the large difference in observed fluxes could only be caused by the individual sedimentary environment of each profile. A much lower average $^{210}Pb_{ex}$ flux of 5.5 and 3.5 Bq/m^2a, in Antarctica was calculated based on the ^{210}Pb concentration in the surface snow and annual mean precipitation (Preiss et al., 1996, Appleby, 2008, Table 5). This flux was more than one order of magnitude lower than the levels in the mid-latitude sites in the Northern Hemisphere, and was in accordance with the simulated results from modeling (Henderson and Maier-Reimer, 2002). As mentioned above, $^{210}Pb_{ex}$ flux in the lacustrine sediments affected by seabirds at Signy Island, Antarctica, was higher than the estimated atmosphere flux (Appleby et al., 1995, Table 5). The phenomenon of amplified sedimentary ^{210}Pb flux was believed to be induced by a concentrated ^{210}Pb from the catchment loads from inflows during the austral spring thaw (Appleby, 2008; Sanders et al., 2010). According to field records (Table 1), MB4 was collected from a lacustrine environment, which receives precipitated ^{210}Pb from the entire catchment. MB1 consisted of dry sediments, but judging from the surrounding terrain, this site should be within or near an aquatic environment. In contrast, MB6 and CC were directly excavated from active penguin colonies with much less inflow than the two profiles mentioned above. Thus, the lower $^{210}Pb_{ex}$ fluxes in MB6 and CC are understandable. However, profile MB1 with its smaller catchment size and lower moisture level than MB4 exhibited higher $^{210}Pb_{ex}$ and ^{137}Cs fluxes in the sediments. This cannot simply be explained by the difference of the depositional environment, for the ^{137}Cs flux in MB1 was more than twice as much as in MB4.

To explore the reason behind this, we plotted $^{210}Pb_{ex}$ and ^{137}Cs flux data of MB1, MB4, MB6 and CC from Ross Island with their average deposition rate (Fig. 3). Combined with the distribution of the sampling sites shown in Fig. 1, the decreasing order of deposition rate from MB1 to CC indicates that the extra nuclides in profile MB1 were highly relevant to its location. Due to the low rain/snow fall in Antarctica (~202.5 mm in McMurdo Sound), melt water from accumulated snow in the glacial fronts becomes the most important supply for the ponds and catchments scattered in the ice-free areas, ensuring the prosperity of the local ecosystem (Kennedy, 1993; Archer et al., 2015). Precipitated ^{210}Pb and ^{137}Cs would be trapped in the permanent ice cover with continuously formed new snow, and partly carried away by the flows of melt water during the thaw in the austral spring (Pourchet et al., 2003; Suzuki et al., 2004). The ice-free area of Cape Bird extends from the coast up to the western margin of the Mt Bird ice cap which feeds

Table 5
Flux of $^{210}Pb_{ex}$ determined on different sources across Antarctica.

Region	Source	Reference	$^{210}Pb_{ex}$ flux (Bq/m^2a)
Ross Sea	Ornithogenic sediment	This study	20.67–87.24
McMurdo Dry Valleys	Lacustrine sediment	Doran et al., 1999	0.15–16.61
Signy Island, Antarctic Peninsula	Lacustrine sediment	Appleby et al., 1995	32–137
South Shetland Islands, Antarctic Peninsula	Lacustrine sediment	Roos et al., 1994	1.25–8.72
60–90° S	Atmospheric precipitation	Preiss et al., 1996	3.5
Antarctica	Atmospheric precipitation	Appleby, 2008	5.5

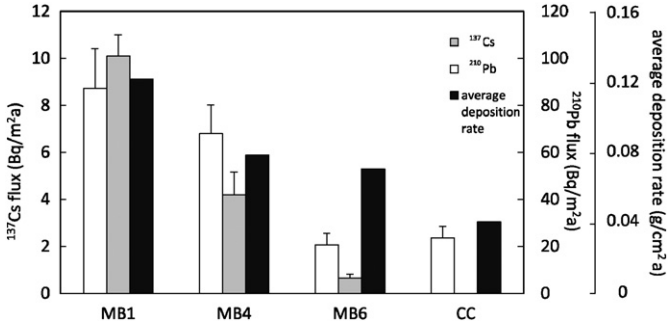

Fig. 3. $^{210}Pb_{ex}$ and ^{137}Cs flux in profile MB1, MB4, MB6 and CC with average deposition rate showing a decreasing trend from glacial front to near-shore penguin colonies.

several outlet glaciers that flow around parasitic cinder cones and terminate on land (Dochat et al., 2000). Judging from the geographic features at Cape Bird and field records, surface runoff from the scattered glacial fronts and snow banks in front of the Mt Bird ice cap would flow from the elevated hillside through raised beach ridges and finally to the sea shore (Fig. 1). Thus the MB1 profile which was closer to the glacial front would receive more inflow, and it was clearly corroborated by its elevated average deposition rate (as high as 0.12 g/cm^{2}a; Fig. 3). MB4 with a larger catchment but farther away from the glacial front, however, has a lower deposition rate, which in turn resulted in lower $^{210}Pb_{ex}$ and ^{137}Cs flux, not to mention MB6 and CC with even smaller catchment sizes and deposition rate. Since the chemical activity and mobility of Cs were much higher than Pb, its downward movement was more significant, resulting in a more drastic decrease from profiles with high to low deposition rates (Ivanovich and Harmon, 1992; Mietelski et al., 2008).

Apart from the different fluxes among profiles, high $^{210}Pb_{ex}$ and ^{137}Cs flux in the site closest to the glacial front may also indicate an increased input of melt water caused by continuous warming over the recent century (Appleby et al., 1995; Gulin and Stokozov, 2005; Sanders et al., 2010). To test this hypothesis, we plotted the deposition rate of the four profiles against age sequence (Fig. 4). As is shown in this figure, the deposition rate of all profiles showed constant ascending trends toward the present, except for the sudden drop in the surface layer in MB1. The curves were rather low and stable before 1960–1970s, and began to rise rapidly thereafter. The most recent one or two decades witnessed the highest deposition rate in this region. According to the report of PAGES 2 k Consortium, synthetic temperature reconstructions using different data sources exhibit a clear warming trend after the Little Ice Age (LIA) in Antarctica. Rhodes et al. (2012) reported that the Ross Sea region was 1.6 ± 1.4 °C warmer in the post-LIA period than during the LIA based on the analyses of δD from an ice core from Mt Erebus (Ross Island) in the Ross Sea region. Similarly, Bertler et al. (2011) reported their isotopic analysis on an ice core retrieved from the Victoria Lower Glacier, showing the surface temperatures in the Ross Sea region increased about 2 °C after the LIA. According to the instrumentally recorded meteorological data from Scott Base on Ross Island, there has been a significant spring warming of 0.41 ± 0.39 °C per decade since 1958, and this trend increased to 0.64 ± 0.69 °C per decade after 1979 (Clark et al., 1988; Schneider et al., 2012; Sinclair et al., 2012). This warming also has been corroborated by the increasing resident Adélie penguin population and the southward expansion of their colonies since the 1970s (Taylor and Wilson, 1990). There is no doubt that the warming in this region would produce more melt water, increase the surface flow carrying the nuclides accumulated in the ice, snow and soil detritus. As our cores were sampled along the runoff pathway, and they have different accumulation rates, this would enhance the difference of the inventories and fluxes of $^{210}Pb_{ex}$ and ^{137}Cs among the profiles (Sanders et al., 2010). Nonetheless, the evident rise of sedimentation rate and flux throughout all sediment profiles is a sound indicator of successive warming over the past century. Thus, it is clear that nuclides in the ornithogenic sediments from the Ross Sea region can be used not only in chronological determinations, but also as indicators for local climate changes.

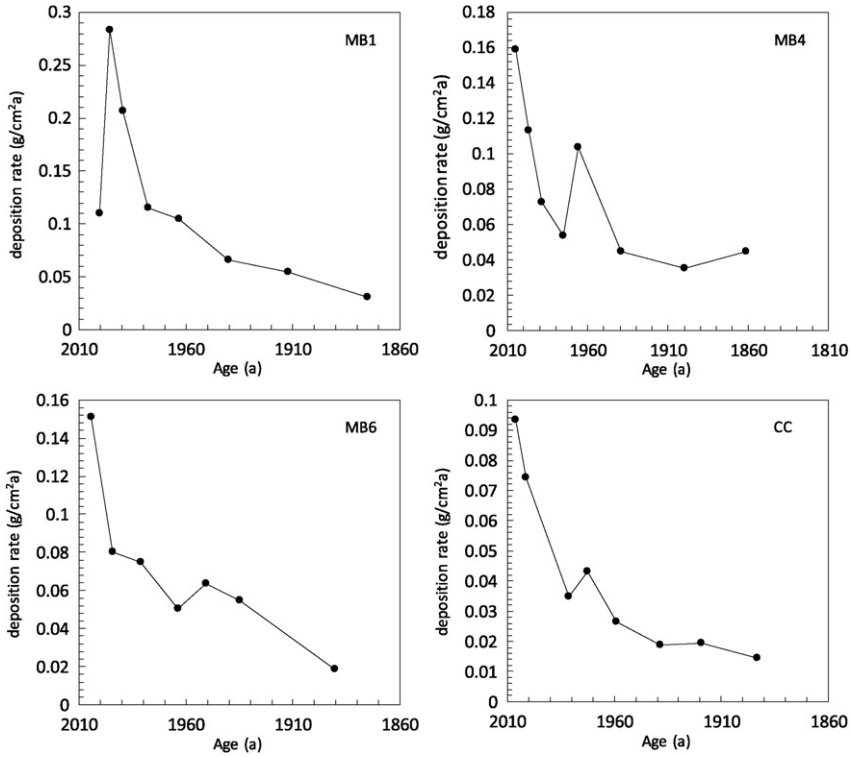

Fig. 4. Deposition rate in the upper layers of profile MB1, MB4, MB6 and CC.

4. Conclusion

Based on the analyses of radionuclides including ^{210}Pb, ^{226}Ra and ^{137}Cs, age sequences from eight ornithogenic sediment profiles were successfully obtained using the CRS model, verifying the reliability of ^{210}Pb dating on this type of geo-carrier heavily influenced by biological activities in the Ross Sea region. The difference of $^{210}Pb_{ex}$ and ^{137}Cs flux among four profiles was found to be influenced by their individual depositional environments. The decreasing flux from MB1 to CC was induced by the different average deposition rate of the sediments, which was related to the specific location of the profiles. The rising deposition rate against age revealed in all four profiles indicated increased runoff of melt water carrying ^{210}Pb and ^{137}Cs from accumulated snow in the warming environment of the last century (especially after the 1970s), which implies the potential of radionuclides as environmental indicators in this region.

Supplementary data to this article can be found online at http://dx.doi.org/10.1016/j.scitotenv.2016.03.046.

Acknowledgements

We would like to thank the Chinese Arctic and Antarctic Administration of the State Oceanic Administration for project support. We also thank the United States Antarctic Program (USAP), Raytheon Polar Services, and in particular J. Smykla, E. Gruber and L. Coats for their valuable assistance in the field. This study was supported by the National Natural Science Foundation of China (Grant Nos. 41576183 and 41376124) and NSF Grant ANT 0739575.

References

Appleby, P.G., 2008. Three decades of dating recent sediments by fallout radionuclides: a review. The Holocene 18 (1), 83–93.
Appleby, P.G., 2000. Radiometric dating of sediment records in European mountain lakes. J. Limnol. 59 (1 s), 1–14.
Appleby, P.G., Oldfield, F., 1978. The calculation of ^{210}Pb dates assuming a constant rate of supply of unsupported lOPb to the sediments. Catena 51-18.
Appleby, P.G., Jones, V.J., Ellis-Evans, J.C., 1995. Radiometric dating of lake sediments from Signy Island (maritime Antarctic): evidence of recent climatic change. J. Paleolimnol. 13 (2), 179–191.
Archer, S.D.J., McDonald, I.R., Herbold, C.W., Lee, C.K., Cary, C.S., 2015. Benthic microbial communities of coastal terrestrial and ice shelf Antarctic meltwater ponds. Front. Microbiol. 6, 485.
Arnaud, F., Magand, O., Chapron, E., Bertrand, S., Boës, X., Charlet, F., Mélières, M.A., 2006. Radionuclide dating (^{210}Pb, ^{137}Cs, ^{241}Am) of recent lake sediments in a highly active geodynamic setting (lakes Puyehue and Icalma—Chilean Lake District). Sci. Total Environ. 366 (2), 837–850.
Bertler, N., Mayewski, P.A., Carter, L., 2011. Cold conditions in Antarctica during the little ice age—implications for abrupt climate change mechanisms. Earth Planet. Sci. Lett. 308 (1), 41–51.
Clarke, A., Holmes, L., White, M., 1988. The annual cycle of temperature, chlorophyll and major nutrients at Signy Island, South Orkney Islands, 1969–82. Br. Antarct. Surv. Bull. 80, 65–86.
Clarke, A., Murphy, E.J., Meredith, M.P., King, J.C., Peck, L.S., Barnes, D.K., Smith, R.C., 2007. Climate change and the marine ecosystem of the western Antarctic Peninsula. Philosophical Transactions of the Royal Society B: Biological Sciences 362 (1477), 149–166.
de Lima Ferreira, P.A., Ribeiro, A.P., do Nascimento, M.G., de Castro Martins, C., de Mahiques, M.M., Montone, R.C., Figueira, R.C.L., 2013. ^{137}Cs in marine sediments of Admiralty Bay, King George Island, Antarctica. Sci. Total Environ. 443, 505–510.
Dochat, T.M., Marchant, D.R., Denton, G.H., 2000. Glacial geology of Cape Bird, Ross Island, Antarctica. Geografiska Annaler. Series A. Physical Geography 237-247.
Doran, P.T., Berger, G., Lyons, W., Wharton, R., Davisson, M., Southon, J., Dibb, J., 1999. Dating quaternary lacustrine sediments in the McMurdo dry valleys, Antarctica. Palaeogeogr. Palaeoclimatol. Palaeoecol. 147 (3), 223–239.
Emslie, S.D., Coats, L., Licht, K., 2007. A 45,000 yr record of Adélie penguins and climate change in the Ross Sea, Antarctica. Geology 35 (1), 61–64.
Gallée, H., Guyomarc'h, G., Brun, E., 2001. Impact of snow drift on the Antarctic ice sheet surface mass balance: possible sensitivity to snow-surface properties. Bound.-Layer Meteorol. 99 (1), 1–19.
Giuliani, S., Triulz, C., Vaghi, M., 2003. Antropogenic radionuclides in plants, animals and their environments in Antarctica. Marine Ecological Journal 2 (2), 5–15.
Godoy, J.M., Schuch, L.A., Nordemann, D.J.R., Reis, V.R.G., Ramalho, M., Recio, J.C., Brito, R.R.A., Olech, M.A., 1998. ^{137}Cs, ^{226,} ^{228}Ra, ^{210}Pb and $^{4°}$K concentrations in Antarctic soil, sediment and selected moss and lichen samples. J. Environ. Radioact. 41 (1), 33–45.
Goldberg, E.D., 1963. Geochronology with ^{210}Pb. Radioactive Dating 121-131.
Goodwin, I.D., 1990. Snow accumulation and surface topography in the katabatic zone of Eastern Wilkes Land, Antarctica. Antarct. Sci. 2 (03), 235–242.
Gulin, S.B., Stokozov, N.A., 2005. ^{137}Cs concentrations in Atlantic and western Antarctic surface waters: results of the 7th Ukrainian Antarctic Expedition, 2002. J. Environ. Radioact. 83 (1), 1–7.
Henderson, G.M., Maier-Reimer, E., 2002. Advection and removal of ^{210}Pb and stable Pb isotopes in the oceans: a general circulation model study. Geochim. Cosmochim. Acta 66 (2), 257–272.
Ivanovich, M., Harmon, R.S., 1992. Uranium-series disequilibrium: applications to earth, marine, and environmental sciences. J. Environ. Radioact. 41 (1), 33–45.
Jenouvrier, S., Barbraud, C., Weimerskirch, H., 2005. Long-term contrasted responses to climate of two Antarctic seabird species. Ecology 86 (11), 2889–2903.
Jia, G., Triulzi, C., Marzano, F.N., Belli, M., Vaghi, M., 2000. The fate of plutonium, ^{241}Am, ^{90}Sr and ^{137}Cs in the Antarctic ecosystem. Antarct. Sci. 12 (02), 141–148.
Kennedy, A.D., 1993. Water as a limiting factor in the Antarctic terrestrial environment: a biogeographical synthesis. Arct. Alp. Res. 308-315.
Koide, M., Michel, R., Goldberg, E.D., Herron, M.M., Langway, C.C., 1979. Depositional history of artificial radionuclides in the Ross Ice Shelf, Antarctica. Earth Planet. Sci. Lett. 44 (2), 205–223.
Krishnaswamy, S., Lal, D., Martin, J., Meybeck, M., 1971. Geochronology of lake sediments. Earth Planet. Sci. Lett. 11 (1), 407–414.
Le Roux, G., Marshall, W., 2011. Constructing recent peat accumulation chronologies using atmospheric fall-out radionuclides. Mires and Peat 7 (1), e14.
Liu, X., Nie, Y., Sun, L., Emslie, S.D., 2013. Eco-environmental implications of elemental and carbon isotope distributions in ornithogenic sediments from the Ross Sea region, Antarctica. Geochim. Cosmochim. Acta 117, 99–114.
Maenhaut, W., Zoller, W.H., Coles, D., 1979. Radionuclides in the South Pole atmosphere. Journal of Geophysical Research: Oceans 84 (C6), 3131–3138 (1978–2012).
McClintock, J., Ducklow, H., Fraser, W., 2008. Ecological responses to climate change on the Antarctic Peninsula. Am. Sci. 96 (4), 302–310.
Mietelski, J., Olech, M., Sobiech-Matura, K., Howard, B., Gaca, P., Zwolak, M., Błażej, S., Tomankiewicz, E., 2008. ^{137}Cs, $^{4°}$K, ^{238}Pu, $^{239+}$ ^{240}Pu and ^{90}Sr in biological samples from King George Island (Southern Shetlands) in Antarctica. Polar Biol. 31 (9), 1081–1089.
Nie, Y., Liu, X., Sun, L., Emslie, S.D., 2012. Effect of penguin and seal excrement on mercury distribution in sediments from the Ross Sea region, East Antarctica. Sci. Total Environ. 433, 132–140.
Nie, Y., Sun, L., Liu, X., Emslie, S., 2015. From warm to cold: migration of Adelie penguins within Cape Bird, Ross Island. Sci. Rep. 5 (11530-11530).
Parmesan, C., 2006. Ecological and evolutionary responses to recent climate change. Annu. Rev. Ecol. Evol. Syst. 637-669.
Pourchet, M., Magand, O., Frezzotti, M., Ekaykin, A., Winther, J.G., 2003. Radionuclides deposition over Antarctica. J. Environ. Radioact. 68 (2), 137–158.
Preiss, N., Mélières, M.A., Pourchet, M., 1996. A compilation of data on lead 210 concentration in surface air and fluxes at the air-surface and water-sediment interfaces. J. Geophys. Res. Atmos. 101 (D22), 28847–28862 (1984–2012).
United Nations Scientific Committee on the Effects of Atomic Radiation, 1982i. Ionizing Radiation: Sources and Biological Effects.
Rhodes, R., Bertler, N., Baker, J., Steen-Larsen, H.C., Sneed, S., Morgenstern, U., Johnsen, S.J., 2012. Little Ice Age climate and oceanic conditions of the Ross Sea, Antarctica from a coastal ice core record. Clim. Past 8 (4), 1223–1238.
Roos, P., Holm, E., Persson, R., Aarkrog, A., Nielsen, S., 1994. Deposition of ^{210}Pb, ^{137}Cs, $^{239+}$ ^{240}Pu, ^{238}Pu, and ^{241}Am in the Antarctic Peninsula area. J. Environ. Radioact. 24 (3), 235–251.
Sanders, C.J., Santos, I.R., Patchineelam, S.R., Schaefer, C., Silva-Filho, E.V., 2010. Recent ^{137}Cs deposition in sediments of Admiralty Bay, Antarctica. J. Environ. Radioact. 101 (5), 421–424.
Schneider, D.P., Deser, C., Okumura, Y., 2012. An assessment and interpretation of the observed warming of West Antarctica in the austral spring. Clim. Dyn. 38 (1–2), 323–347.
Schüller, P., Bunzl, K., Voigt, G., Ellies, A., Castillo, A., 2004. Global fallout ^{137}Cs accumulation and vertical migration in selected soils from South Patagonia. J. Environ. Radioact. 71 (1), 43–60.
Sinclair, K.E., Bertler, N.A., Van Ommen, T.D., 2012. Twentieth-century surface temperature trends in the western Ross Sea, Antarctica: evidence from a high-resolution ice core. J. Clim. 25 (10), 3629–3636.
Suzuki, T., Kamiyama, K., Furukawa, T., Fujii, Y., 2004. Lead-210 profile in firn layer over Antarctic ice sheet and its relation to the snow accumulation environment. Tellus B 56 (1), 85–92.
Taylor, R., Wilson, P., 1990. Recent increase and southern expansion of Adelie penguin populations in the Ross Sea, Antarctica, related to climatic warming. N. Z. J. Ecol. 25–29.
Xu, L., Liu, X., Sun, L., Yan, H., Liu, Y., Luo, Y., Huang, J., Wang, Y., 2010. Distribution of radionuclides in the guano sediments of Xisha Islands, South China Sea and its implication. J. Environ. Radioact. 101 (5), 362–368.